Does Taper Angle Clearance Influence Fretting and Corrosion Damage at the Head-Stem Interface? A Matched Cohort Retrieval Study

Sevi B. Kocagöz, BS[1], **Richard J. Underwood, PhD**[1,2], **Shiril Sivan, BE**[3,4], **Jeremy L. Gilbert, PhD**[3,4], **Daniel W. MacDonald, MS**[1], **Judd S. Day, PhD**[1,2], and **Steven M. Kurtz, PhD**[1,2]

[1]School of Biomedical Engineering, Science, and Health Systems, Drexel University, Philadelphia PA

[2]Exponent Inc., Philadelphia PA

[3]Syracuse Biomaterials Institute, Syracuse University, Syracuse, NY

[4]Department of Biomedical and Chemical Engineering, Syracuse University, Syracuse NY

Abstract

Corresponding Author: Steven M. Kurtz, Ph.D., *Research Professor*, School of Biomedical Engineering, Science & Health Systems, Drexel, University, Philadelphia PA, *Director*, Implant Research Center at Drexel University, 3401 Market St. Suite 345, Philadelphia, PA 19104, smk38@drexel.edu.
The work reported in this paper was completed at the Implant Research Center at Drexel University (Philadelphia, PA) and Syracuse Biomaterials Institute, Syracuse University (Syracuse, NY). For first proofs and for reprint requests please contact the Implant Research Center at Drexel University, 3401 Market St. Suite 345, Philadelphia, PA 19104. Phone: (215) 571 4347. sk997@drexel.edu.
Sevi B. Kocagöz, B.S., *Ph.D. Candidate*, Implant Research Center at Drexel University, School of Biomedical Engineering, Science, and Health Systems, Drexel University, 3401 Market St. Suite 345, Philadelphia, PA 19104, Phone: (215) 571 4347, Fax: (215) 571 4348, sk997@drexel.edu
Richard J. Underwood, Ph.D., *Visiting Research Professor*, School of Biomedical Engineering, Science, and Health Systems, Drexel University, 3141 Chestnut Street, Philadelphia, PA 19104, Phone: (215) 895-2215, Fax: (215) 895-4983
Associate, Exponent Inc., Philadelphia PA, 3440 Market St. Suite 600, Philadelphia, PA 19104, Phone: (215) 594-8875, Fax: (215) 594-8899, runderwood@exponent.com
Judd S. Day, Ph.D., *Research Assistant Professor*, School of Biomedical Engineering, Science, and Health Systems, Drexel University, 3141 Chestnut Street, Philadelphia, PA 19104, Phone: (215) 895-2215, Fax: (215) 895-4983
Managing Scientist, Exponent Inc., Philadelphia PA, 3440 Market St. Suite 600, Philadelphia, PA 19104, Phone: (215) 594-8834, Fax: (215) 594-8899, jday@exponent.com
Daniel W. MacDonald, M.S., *Ph.D. Candidate*, Implant Research Center at Drexel University, School of Biomedical Engineering, Science, and Health Systems, Drexel University, 3401 Market St. Suite 345, Philadelphia, PA 19104, Phone: (215) 571 4347, Fax: (215) 571 4348, dm68@drexel.edu
Shiril Sivan, BE, *Ph.D. Candidate*, Department of Biomedical and Chemical Engineering, Syracuse Biomaterials Institute, 318 Bowne Hall, Syracuse University, Syracuse, NY 13244, Phone: (315) 443-3500, ssivan@syr.edu
Jeremy L. Gilbert, Ph.D., FBSE, *Professor of Biomaterials, Editor-in-Chief*, Journal of Biomedical Materials Research – Part B: *Applied Biomaterials*, Department of Biomedical and Chemical Engineering, Syracuse Biomaterials Institute, 303C Bowne Hall, Syracuse University, Syracuse, NY 13244, Phone: (315) 443-2105, gilbert@syr.edu
Steven M. Kurtz, Ph.D., *Research Professor*, School of Biomedical Engineering, Science & Health Systems, Drexel, University, Philadelphia PA, *Director*, Implant Research Center at Drexel University, 3401 Market St. Suite 345, Philadelphia, PA 19104, smk38@drexel.edu
Corporate Vice President and Practice Director, Exponent Inc., Philadelphia, 3440 Market St. Suite 600, Philadelphia, PA 19104, Phone: (215) 594-8851, Fax: (215) 594-8899, skurtz@exponent.com

Disclosures
The following authors have no conflict of interest to disclose: Sevi B. Kocagöz, Shiril Sivan, Daniel W. Macdonald

Previous studies have speculated that modular taper design may have an effect on the corrosion and material loss at the taper surfaces. We present a novel method to measure taper angle for retrieved head taper and stem trunnions using a roundness machine (Talyrond 585, Taylor Hobson, UK). We also investigated the relationship between taper angle clearance and visual fretting-corrosion score at the taper-trunnion junction using a matched cohort study of 50 ceramic and 50 metal head-stem pairs. In this study, no correlation was observed between the taper angle clearance and the visual fretting-corrosion scores in either the ceramic or the metal cohorts.

Introduction

Release of metallic wear and corrosion products from the modular connections of total hip arthroplasties (THA) has recently emerged as a clinical concern [1–4]. Investigations of taper corrosion have shown that a combination of mechanical, electrochemical, geometrical, material and chemical conditions at the taper junctions affect taper corrosion [5–7]. Previous studies have highlighted several factors, such as lower neck flexural rigidity, increased modularity, external environment during assembly, and impaction forces may be associated with fretting and corrosion damage [8–13]. Previous research has also suggested that ceramic femoral heads mitigate taper fretting-corrosion between the head taper and the stem trunnion [14,15].

Modular junction design, including angular mismatch and conicity [9], has been hypothesized as an additional factor that may minimize the generation of corrosion products [16,17]. However, little is known about the effect of head taper and stem trunnion angles and their potential effect on taper damage [18–20]. The contact mechanics of the taper-trunnion junction may be influenced in part by the angular mismatch between the head and the trunnion, as well as other variables of the head-neck interface [20]. Two previous explant studies, neither of which actually measured taper angle clearance in their retrieved components, have speculated that angular clearance may contribute to material loss at the taper-trunnion junction [21,22].

The overall goal of the present study was to investigate the hypothesized relationship between taper angle clearance and fretting-corrosion damage in stems mated with ceramic and metal heads. Building on our previously assembled cohorts of ceramic head and metal head retrievals [14], we asked (1) whether a novel methodology for characterizing the taper angle clearance in retrieved heads and stem pairs would be sufficiently repeatable and reproducible to accurately measure the explanted components; (2) if there was a difference in clearance angle and contact location between the ceramic and metal cohorts; (3) did taper angle clearance help explain the variability in the extent and severity of taper damage in the ceramic and metal cohorts; and (4) was there evidence of wear/corrosion in taper regions identified with material loss?

Materials and Methods

Study Design, Cohort Selection, and Clinical Information

Components were selected from the retrieval collections of two academic engineering-based programs working in collaboration with 12 clinical revision centers around the United States as part of a 12-year ongoing institutional review board approved revision and retrieval program. In our previous study [14], an *a priori* power analysis revealed that a total sample size of 100 would be adequate to detect a difference in visual fretting-corrosion score of 1 on a scale of 1–4 between the ceramic and metal cohorts. For the current study, we continued our previous study by measuring the taper angle clearance in the same matched

cohorts of 50 ceramic and 50 metal head-stem pairs because it allowed us to isolate and investigate taper angle clearance for the present study.

Taper and Trunnion Angle Measurements

In this study, we define the taper angle as twice the measured half angle of the geometric cone forming the head taper or stem trunnion. Taper angle clearance is the difference between the head taper angle and trunnion angle:

Taper angle clearance = Taper angle of head – trunnion angle of stem

Positive clearance, which will result in proximal contact between the head and trunnion, occurs when the taper angle is greater than the trunnion angle. Negative clearance, on the other hand, will result in distal contact (Figure 1).

The head and trunnion taper angles were measured using a roundness machine (Talyrond 585, Taylor Hobson, UK), equipped with a diamond or ruby stylus. The component was mounted in a custom fixture on the Talyrond rotating stage and the angular position was referenced against a landmark (e.g. laser etched markings) on the component. The component was centered and leveled using measurements in the as-manufactured regions (Figure 2) to align the axis of symmetry of the machine with the axis of rotation of the component. The as-manufactured surfaces were identified by visual inspection of the taper surface and 4 axial profiles, measured at 90° intervals around the taper. After centering and leveling, an axial profile was measured over the top edge of the taper to establish a height datum. A series of 5 to 7 circumferential profiles were measured in the identified as-manufactured region(s) of the taper surface, typically spaced at a vertical distance of 1 – 3 mm. The number and spacing of the profiles depended on the length of the taper and the location and size of the as-manufactured regions. The head tapers were measured using a diamond stylus with a tip radius of 5 μm. Due to the presence of microgrooves and sometimes extensive iatrogenic damage, a 4-mm diameter ruby stylus was used to measure the surface of all trunnions to prevent damage to the diamond tip and provide mechanical filtering of the microgrooves. Each roundness profile was analyzed using Ultra software [Taylor Hobson, UK] and a least-squares (LS) circle was fitted. The LS fit was improved by excluding regions of asymmetric wear or point defects. For consistency, it was required that after exclusions, at least 55% of the profile was used in the fit and the deviation of the points in each remaining profile was less than 10 μm. A second skilled operator identified the as-manufactured regions for each component and cross-checked for agreement of the selected vertical height location and exclusions applied on each roundness profile. The radius and height of each LS circle was compiled in a spreadsheet and the linear slope of the radius of the 5–7 profiles was used to calculate the taper angle (Figure 3). Repeatability measurements for taper angle were performed using both the diamond and ruby styli on a reference taper ring gauge. The diamond stylus is used for taper angle measurements because of higher resolution and the 4 mm ruby stylus is used for trunnion angle measurements to prevent damage to the diamond stylus from the as manufacture grooves on some of the trunnions.

Repeatability Study

A repeatability study was conducted to characterize the uncertainty in the taper and trunnion angle measurements. Repeatability of angle measurements using the Talyrond for as manufactured surfaces was validated with a study conducted using a precision tapered ring gauge. Twenty-five angle measurements were performed on different days, and using both the diamond and ruby stylus.

Surface Topography Characterization

The regions with material loss were identified by the axial Talyrond profiles and visual inspection. Twenty-four female metal taper surfaces showed evidence of material loss and thirteen were inspected using scanning electron microscopy (SEM, JEOL JSM-5600) and an optical microscope (KH-8700, HIROX) for evidence of fretting-corrosion mechanisms (up to 320×). The thirteen representative components selected for imaging had the most severe cases of corrosion. Representative Talyrond profiles showing material removal can be seen in Figure 4. Backscatter electron composition (BEC) images are used to inspect surfaces during SEM imaging because the intensity of the backscattered electron signal is related to the atomic number of the entities being imaged. Using BEC allowed differentiation between the accumulated biological and corrosion deposits and the electrochemical/mechanical topography changes on the metal surfaces being imaged.

Results

The standard deviation of the repeatability study was 13.3 seconds. By contrast, a previous explant study [18] has measured the range of head taper angles in retrieved implants and reported a variation of 0.23 degrees (13.8 minutes). Two stems had extensive iatrogenic damage, preventing accurate trunnion angle measurements and thus, 2 head-stem pairs had to be removed from the study.

Taper angle measurements for ceramic and metal heads resulted in no overlap between the taper and trunnion angles in the ceramic cohort, while there was overlap in the metal cohort (Figure 5). Hence, calculation of taper angle clearance revealed a difference between the ceramic and metal cohorts. The ceramic cohort had exclusively positive taper angle clearance, geometrically indicating proximal contact (Figure 1). The metal taper cohort had both positive (n=35) (proximal) and negative (n=15) (distal) taper angle clearance (Figure 6). Proximal contact in the ceramic cohort was further verified visually by evidence of metal transfer at the proximal end of the head taper (Figure 7). For metal head-stem pairs, it was possible to confirm proximal or distal contact by inspecting the surface topography of measured profiles when there was observable material loss, as determined by a skilled operator who could identify deviations in topography in profiles. Profiles of metal heads showed one of the following wear conditions: a pristine surface with no detectable material loss (n= 32), region with material loss indicating proximal contact (n = 3), distal contact (n = 9), or proximal and distal contact simultaneously (n = 6) (Figure 4).

There was no significant correlation observed between taper angle clearance and visual fretting-corrosion scores for trunnions in the ceramic cohort ($\rho = -0.17$), trunnions in the metal cohort ($\rho = 0.24$) nor the femoral head tapers in the metal cohort ($\rho = -0.05$) (Figure 8). Additionally, visual fretting-corrosion scores in the metal cohort were similar between components with distal contact (negative taper angle clearance) and components with proximal contact (positive taper angle clearance) ($p = 0.43$ and 0.56 for taper and trunnion scores, respectively; Wilcoxon Test).

SEM imaging for metal female tapers with evidence of material loss proximally, distally, or both on measured profiles showed features which are consistent with the findings reported in other studies which identified mechanically assisted corrosion (Figures 9–10) [23,24]. SEM also evidenced that electrochemical material loss (pitting) preferentially evolved in regions that showed evidence of fretting (scratches in the scale 5–40 μm) or had larger scratches (50–500 μm) (Figure 10). We hypothesize that these larger scratches may have been caused when the head was impacted onto the trunnion during the primary surgery or during removal. Local changes in the surface topography were observed in heads mated with both "microgrooved" and "smooth" trunnions (Figure 11–12). The measured profiles and SEM

images of the head taper (Figures 12 and 13) both showed changes in surface topography (the amplitude and wavelength of circumferential grooves) consistent with the microgrooves found on the trunnions – suggesting that "imprinting" had occurred.

Discussion

In this study we investigated the effect of the taper angle clearance (defined as the difference in angle between the head taper and stem trunnion) on the visual fretting and corrosion damage score of a cohort of ceramic and metal tapers. For both the ceramic and the metal head cohorts, the results of this study did not support the hypothesis that taper angle clearance is associated with fretting and corrosion damage of the head or the taper. Factors other than taper angle clearance explain the variation in fretting and corrosion scores between ceramic and CoCr alloy femoral heads.

We would like to highlight some limitations of this study for the reader. First, the taper angles and tolerances reflect matched heads and stems that were designed for compatibility by their respective manufacturer. The study did not include "mixed and matched" heads and stems in which the head of one manufacturer is placed on the stem of another, such as may occur during a revision surgery with limited availability of implant inventory. Second, the stems in this study were all of a monoblock design, such that the only source of modularity was at the head-stem interface. The results of this study, therefore, should not be generalized to head stem designs with additional modular taper connections.

A third limitation of the study was the semi-quantitative, 4-point visual score for assessing the severity of fretting and corrosion. The scoring method was modified from the Goldberg method [9], which is widely used in the literature. This visual assessment does not provide an objective measure of the volume of material lost from the taper surface. Our previous study has shown that there was a correlation between the visual corrosion score and volume of material loss, but it was also shown that there was a large range in the volume of material lost from tapers with the same corrosion score [25]. These results indicated that the visual corrosion scoring method is suitable for preliminary categorization of taper damage, but does have some limitations. A method is being developed to quantitatively measure the volume of material loss and will be presented in a future study.

Another limitation was the small remaining band of as-manufactured taper surface in some femoral head tapers, typically found at the distal end of the head taper. For the current study, the minimum height of this band was 3 mm. The uncertainty in the calculated taper angle will increase as the total distance between the circumferential profiles used to calculate the angle decreases. The uncertainty of using a narrow band of as manufactured surface compared to using a wider band to calculate the taper angle can be estimated. The positional uncertainty of the radial arm and Z-column of the Talyrond is ±0.25 μm. If the taper angle were to be calculated from two measurements, with a radial and height uncertainty of ±0.25 μm, the uncertainty for taper angle is ±0.01° (± 36 seconds) for profiles spaced 3mm apart and ±0.0019° (± 6.8 seconds) for profiles spaced 16 mm apart. This uncertainty is decreased by taking a minimum of 5 circumferential profiles in the as manufactured surfaces. The R-squared value of the data points used to calculate the head angle (Figure 3) was at least 0.9999 or better for all tapers.

This study presented an accurate and repeatable method to measure taper angle and calculated taper angle clearance from retrieved femoral heads and stem trunnions. To the authors' knowledge, this is the first study to report the measurement of the taper and trunnion angles of retrieved femoral head and stem pairs using a roundness machine. Roundness machines are widely used in other industries, such as automotive and bearing, to

measure the geometry of precision tapered components. The accuracy and repeatability of our method was validated with a study conducted using a precision tapered ring gauge for angle measurements on an as-manufactured surface using the Talyrond on different days. For the retrieved implants in our study, repeated measurement and analysis of components identified as outliers, showed reproducibility within the machine uncertainty range.

The results of our study showed that the ceramic cohort had exclusively proximal contact. This is consistent with the design rationale for ceramic femoral heads, in which the angles of the head taper and stem trunnion are specified so that contact occurs at the center of the head where the material cross-section is largest to resist tensile hoop stresses [26]. The metal cohort showed contact at both the distal and proximal end. The metal cohort showed contact at both the distal and proximal end, however, the different contact patterns did not appear to affect the visual fretting-corrosion scores at the head or the trunnion. The simultaneous presence of proximal and distal material loss observed on some metal tapers may indicate toggling motion [22], however, the identification of the mechanism leading to material loss was beyond the scope of this study.

Components with visible distal, proximal and dual contact were examined using SEM to investigate evidence of corrosion in regions of material loss. The investigated components suggest that the imaged mechanical and electrochemical alterations to surface topography correspond to locations of material loss observed in measured profiles. However, further study is needed to understand the mechanism of material loss. For this study, only head taper surfaces were imaged under the SEM and trunnions will be investigated in future work. However, previous investigators have observed significant material loss at the head taper and not at the trunnion [22,27] or that head tapers tended to be corroded more severely than trunnions [9]. Analysis of the measured profiles and SEM images for some metal femoral head tapers, showed a change in surface topography that was consistent with the topography of the microgrooves on the trunnion (Figure 13). This apparent "imprinting" may suggest preferential material loss from the female taper, also reported in previous studies [18,22,27].

In summary, taper angle clearance was not correlated with the visual fretting-corrosion scores in the ceramic or metal cohort in the present study. Research is underway to better characterize the volume of material release from explants to better understand the reasons for reduced fretting and corrosion previously observed in the ceramic femoral head cohort.

Acknowledgments

References

1. Chana R, Esposito C, Campbell PA, Walter WK, Walter WL. Mixing and matching causing taper wear: corrosion associated with pseudotumour formation. J Bone Jt Surg Br. 2012; 94:281–286.

2. Gill IP, Webb J, Sloan K, Beaver RJ. Corrosion at the neck-stem junction as a cause of metal ion release and pseudotumour formation. J Bone Jt Surg Br. 2012; 94:895–900.

3. Meneghini RM, Hallab NJ, Jacobs JJ. Evaluation and treatment of painful total hip arthroplasties with modular metal taper junctions. Orthopedics. 2012; 35:386–391. [PubMed: 22588392]

4. Meyer H, Mueller T, Goldau G, Chamaon K, Ruetschi M, Lohmann CH. Corrosion at the cone/taper interface leads to failure of large-diameter metal-on-metal total hip arthroplasties. Clin Orthop Relat Res. 2012; 470:3101–3108. [PubMed: 22864616]

5. Gilbert, J.; Jacobs, J. The mechanical and electrochemical processes associated with taper fretting crevice corrosion: a review. In: Marlowe, D.; Parr, J.; MB, M., editors. Modul. Orthop. Impants, STP 1301. Vol. vol. 45–59. Conshohocken, PA, USA: ASTM; 1997.

6. Jacobs JJ, Gilbert JL, Urban RM. Corrosion of metal orthopaedic implants. J Bone Jt Surg Am. 1998; 80:268–282.

7. Swaminathan V, Gilbert JL. Fretting corrosion of CoCrMo and Ti6Al4V interfaces. Biomaterials. 2012; 33:5487–5503. [PubMed: 22575833]

8. Collier JP, Surprenant VA, Jensen RE, Mayor MB, Surprenant HP. Corrosion between the components of modular femoral hip prostheses. J Bone Jt Surg Br. 1992; 74:511–517.

9. Goldberg JR, Gilbert JL, Jacobs JJ, Bauer TW, Paprosky W, Leurgans S. A multicenter retrieval study of the taper interfaces of modular hip prostheses. Clin Orthop Relat Res. 2002:149–161. [PubMed: 12151892]

10. Huot Carlson JC, Van Citters DW, Currier JH, Bryant AM, Mayor MB, Collier JP. Femoral stem fracture and in vivo corrosion of retrieved modular femoral hips. J Arthroplast. 2012; 27:1389–1396. e1.

11. Jauch SY, Huber G, Hoenig E, Baxmann M, Grupp TM, Morlock MM. Influence of material coupling and assembly condition on the magnitude of micromotion at the stem-neck interface of a modular hip endoprosthesis. J Biomech. 2011; 44:1747–1751. [PubMed: 21531416]

12. Mroczkowski ML, Hertzler JS, Humphrey SM, Johnson T, Blanchard CR. Effect of impact assembly on the fretting corrosion of modular hip tapers. J Orthop Res. 2006; 24:271–279. [PubMed: 16435360]

13. Pennock AT, Schmidt AH, Bourgeault CA. Morse-type tapers: factors that may influence taper strength during total hip arthroplasty. J Arthroplast. 2002; 17:773–778.

14. Kurtz SM, Kocagoz SB, Hanzlik JA, Underwood RJ, Gilbert JL, Macdonald DW, et al. Do Ceramic Femoral Heads Reduce Taper Fretting Corrosion in Hip Arthroplasty? A Retrieval Study. Clin Orthop Relat Res. 2013; 471:3270–3282. [PubMed: 23761174]

15. Hallab NJ, Messina C, Skipor A, Jacobs JJ. Differences in the fretting corrosion of metal-metal and ceramic-metal modular junctions of total hip replacements. J Orthop Res. 2004; 22:250–259. [PubMed: 15013082]

16. Brown SA, Flemming CA, Kawalec JS, Placko HE, Vassaux C, Merritt K, et al. Fretting corrosion accelerates crevice corrosion of modular hip tapers. J Appl Biomater. 1995; 6:19–26. [PubMed: 7703534]

17. Urban RM, Gilbert JL, Jacobs JJ. Corrosion of Modular Titanium Alloy Stems in Cementless Hip Replacement. J ASTM Int. 2005; 2:215–224.

18. Langton DJ, Sidaginamale R, Lord JK, Nargol AV, Joyce TJ. Taper junction failure in large-diameter metal-on-metal bearings. Bone Jt Res. 2012; 1:56–63.

19. Nassif NA, Nawabi DH, Stoner K, Elpers M, Wright T, Padgett DE. Taper Design Affects Failure of Large-head Metal-on-metal Total Hip Replacements. Clin Orthop Relat Res. 2013

20. Donaldson, FE.; Coburn, JC.; Siegel, KL. Orthop. Res. Soc. Annu. Meet. San Antonio, TX: 2013. Modern taper and trunnion designs may increase taper fretting wear in THA systems.

21. Cook RB, Bolland BJ, Wharton JA, Tilley S, Latham JM, Wood RJ. Pseudotumour formation due to tribocorrosion at the taper interface of large diameter metal on polymer modular total hip replacements. J Arthroplast. 2013; 28:1430–1436.

22. Bishop N, Witt F, Pourzal R, Fischer A, Rutschi M, Michel M, et al. Wear patterns of taper connections in retrieved large diameter metal-on-metal bearings. J Orthop Res. 2013; 31:1116–1122. [PubMed: 23440943]

23. Gilbert JL, Buckley CA, Jacobs JJ. In vivo corrosion of modular hip prosthesis components in mixed and similar metal combinations. The effect of crevice, stress, motion, and alloy coupling. J Biomed Mater Res. 1993; 27:1533–1544. [PubMed: 8113241]

24. Goldberg JR, Buckley CA, Jacobs JJ, Gilbert JL. Corrosion testing of modular hip implants. ASTM Spec. Tech. Publ. 1997; vol. 1301:157–176.

25. Kocagöz, SB.; Underwood, RJ.; MacDonald, DW.; Higgs, GB.; Day, JS.; Siskey, RL., et al. Orthop. Res. Soc. San Antonio, TX, USA: 2013. Does Visual Inspection of the Taper Head / Stem Junctions in Metal-on-Metal Hips Adequately Characterize Material Loss from Corrosion and Wear?.

26. Huet R, Sakona A, Kurtz SM. Strength and reliability of alumina ceramic femoral heads: Review of design, testing, and retrieval analysis. J Mech Behav Biomed Mater. 2011; 4:476–483. [PubMed: 21316636]

27. Matthies AK, Racasan R, Bills P, Blunt L, Cro S, Panagiotidou A, et al. Material loss at the taper junction of retrieved large head metal-on-metal total hip replacements. J Orthop Res. 2013; 31:1677–1685. [PubMed: 23918742]
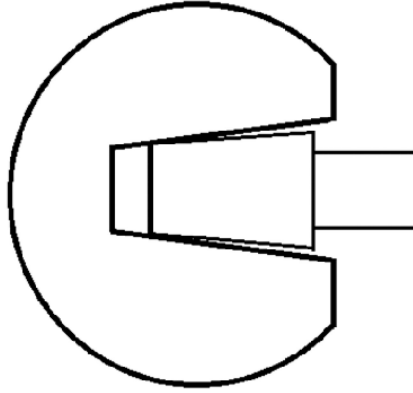
a) Proximal Contact
[taper angle > trunnion angle
Clearance (taper angle – trunnion angle) > 0]
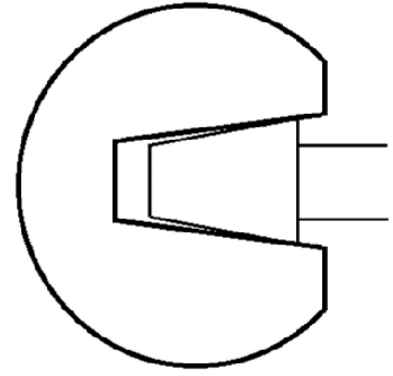
b) Distal Contact
[taper angle < trunnion angle
Clearance (taper angle – trunnion angle) < 0]

Figure 1.
Schematic diagram showing the taper angle clearance, a) shows positive taper angle clearance and proximal head/stem contact, b) shows negative taper angle clearance and distal head/stem contact. These figures are only representatives of the theoretical contact at the taper-trunnion junction. In vivo, while the overall contact area will be located proximally or distally, the contact surfaces may not be axisymmetric and may have a contact area larger on the superior or inferior side with only a point contact on the other side.
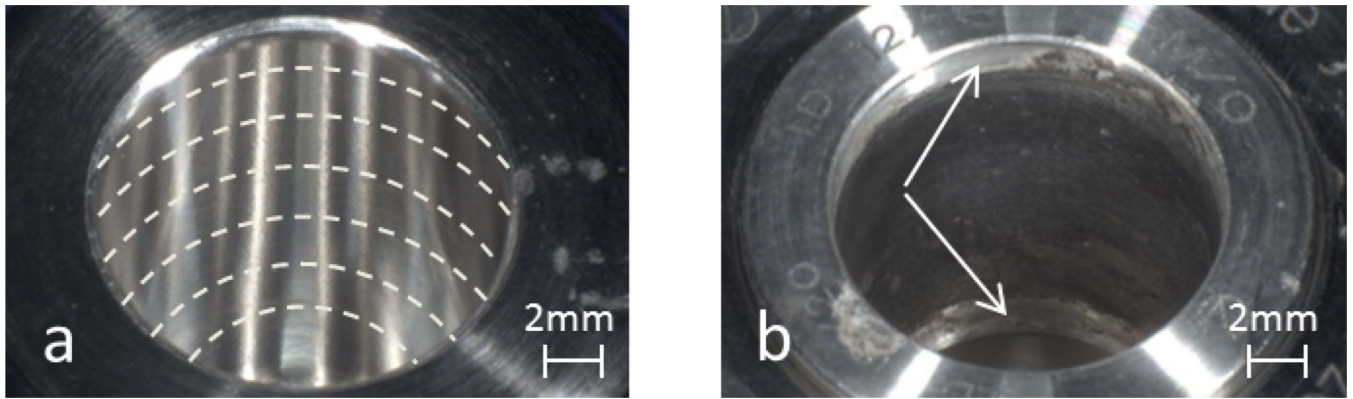
Figure 2.
Figures showing the regions used for measurements in female tapers. a) Taper with visual corrosion score of 1 (Fretting on < 10% surface and no corrosion damage) with profile measured (white dotted lines) evenly spaced throughout taper. b) Taper with corrosion score of 4 (Damage over majority (>50%) of mating surface with severe corrosion attack and abundant corrosion debris) showing identified bands of as manufactured surface remaining at the proximal and distal end of the taper, shown by arrows. The roundness measurements were distributed within these as manufactured surfaces.
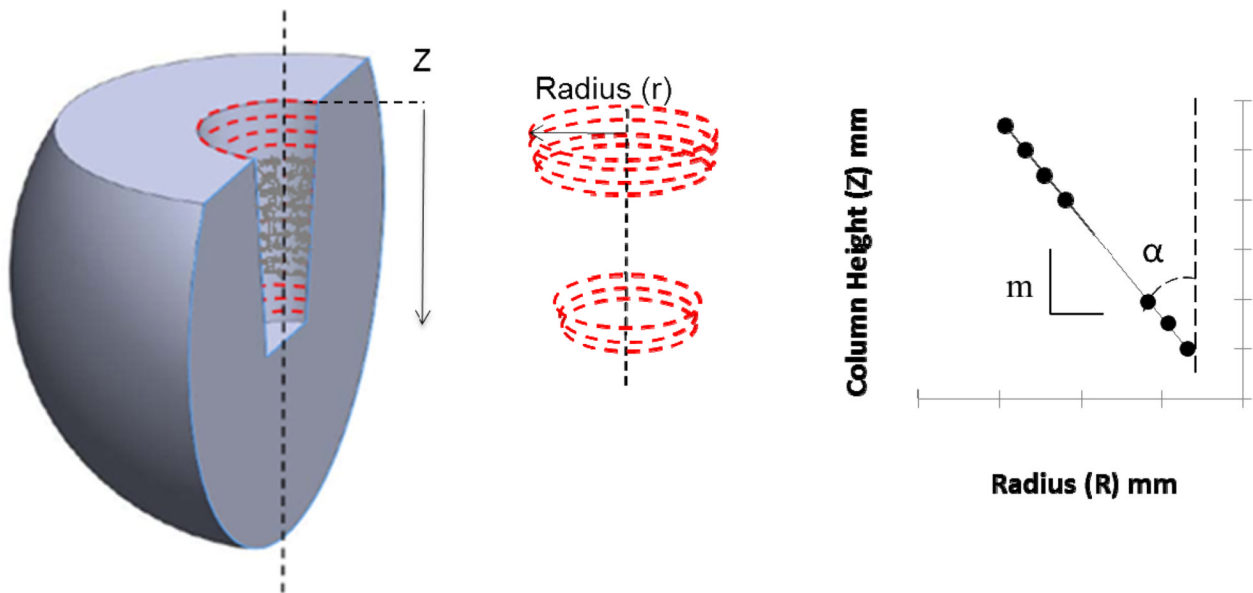
Figure 3.
The radius and relative height of each LS circle was compiled in a spreadsheet and the linear slope of the 5–7 profiles were used to calculate the angle.

$$Taper\ Angle = 2\alpha = 2 \cdot tan^{-1}(-\frac{1}{m}).$$
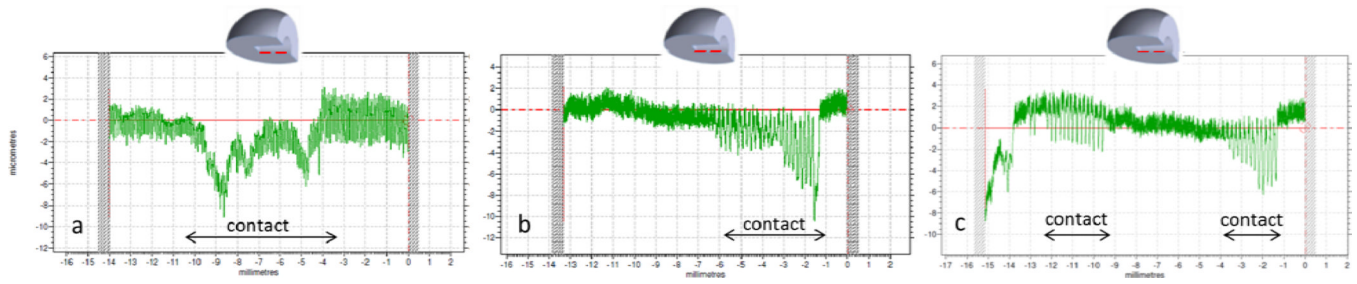
Figure 4.
Examples of Talyrond traces for components with observable regions of material loss proximally (a), distally (b) and in both proximal and distal locations (c). The red lines on the schematic of the femoral heads represent the orientation of the profiles being measured. These profiles provide information about the taper-trunnion junction in addition to the clearance values observed for the metal cohort.
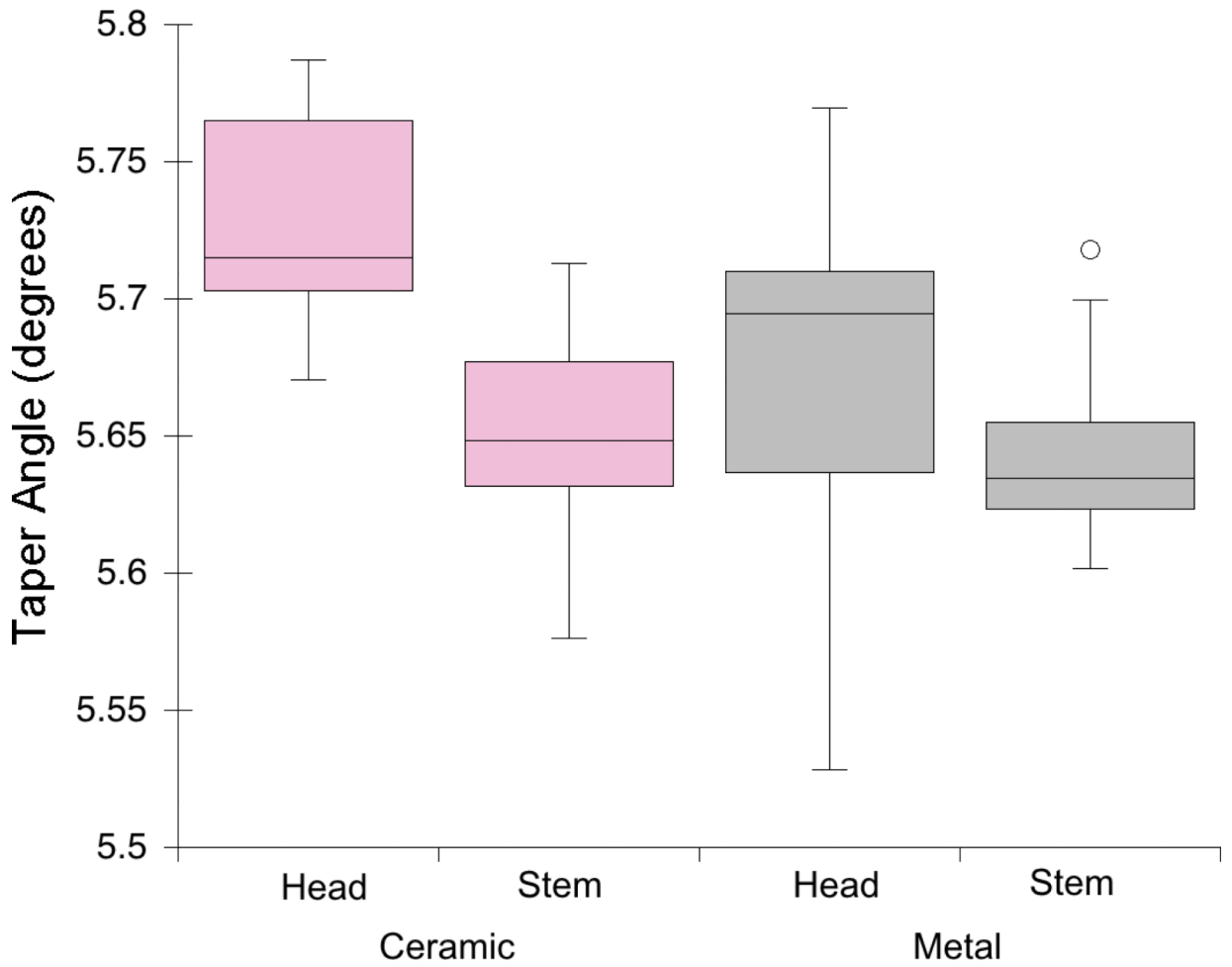
Figure 5.
Taper angle measurements for the ceramic and metal head-stem pairs. There is no overlap in the taper and trunnion angle measurements for the ceramic cohort, while there is overlap in the metal cohort.
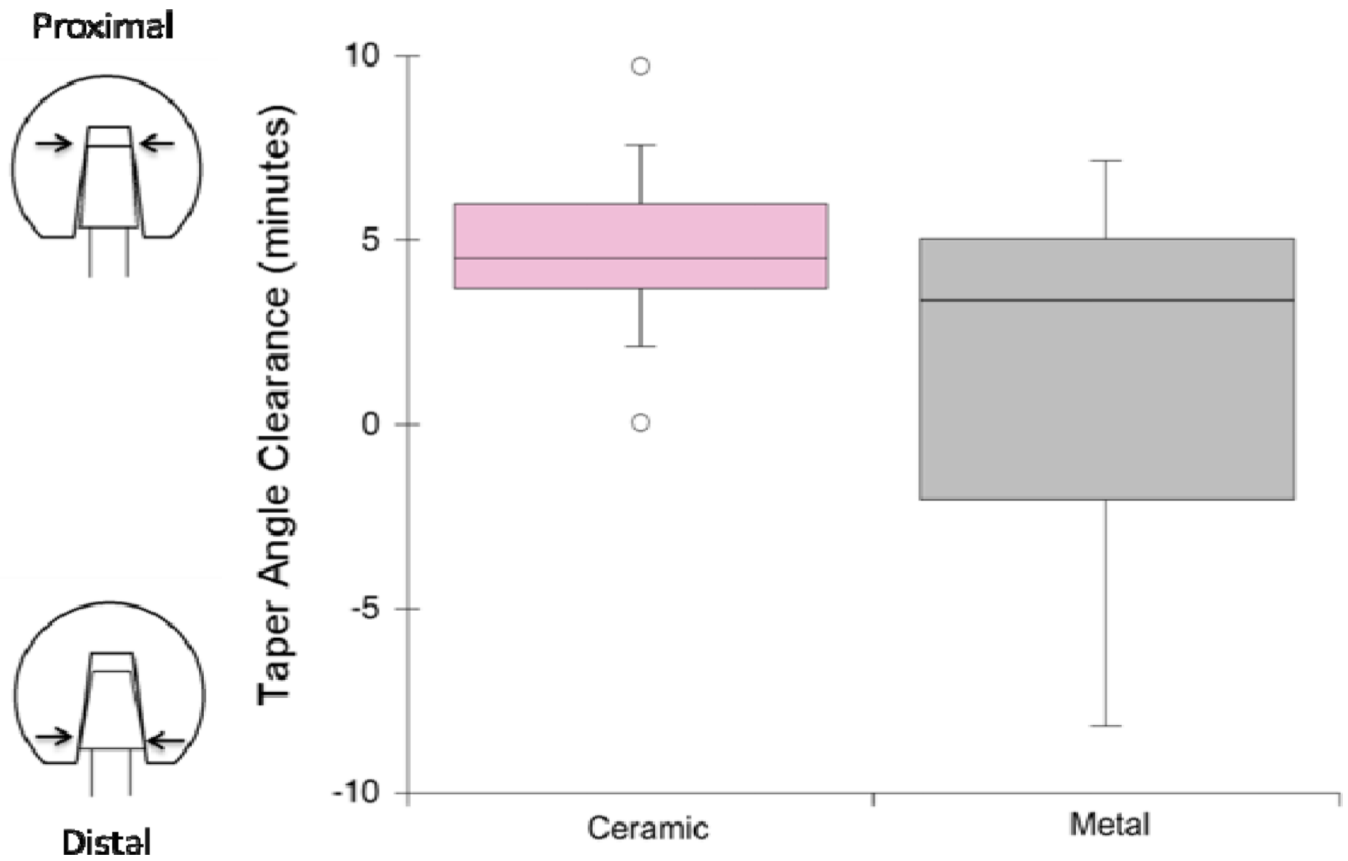
Figure 6.
Taper angle clearance distribution for the ceramic and metal cohorts. The taper angle clearance for the ceramic cohort is always greater than zero (indicating proximal contact), while the metal cohort has clearance values that are greater and smaller than zero (indicating a mixture of proximal and distal contact)

Figure 7.
Metal transfer was observed on the proximal ends of the internal tapers of ceramic heads,
providing visual confirmation for clearance values greater than zero for the ceramic cohort.
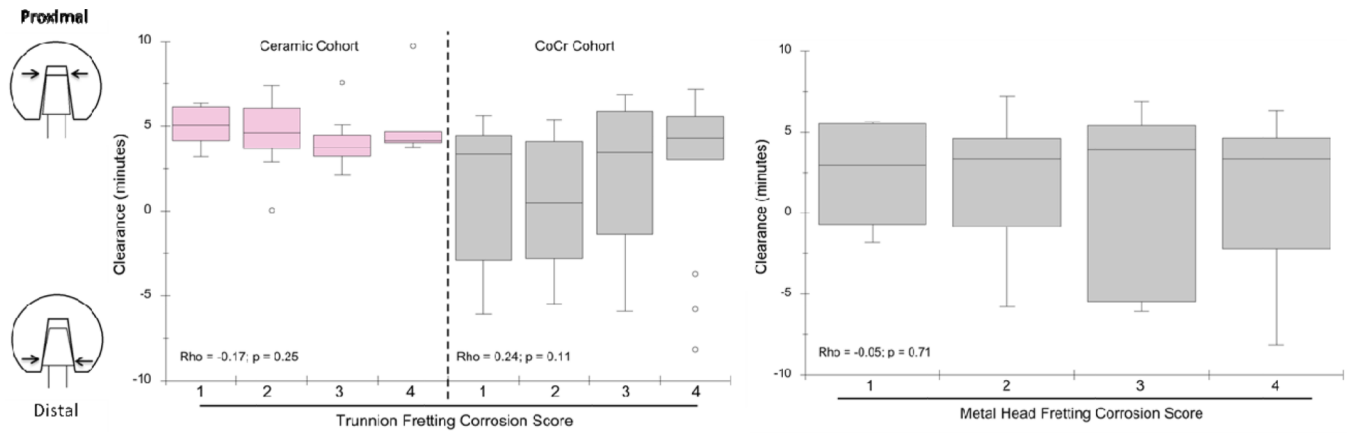
Figure 8.
Distribution of measured ceramic and metal cohorts according to a) trunnion fretting corrosion score, and metal cohort according to b) metal head fretting corrosion score.
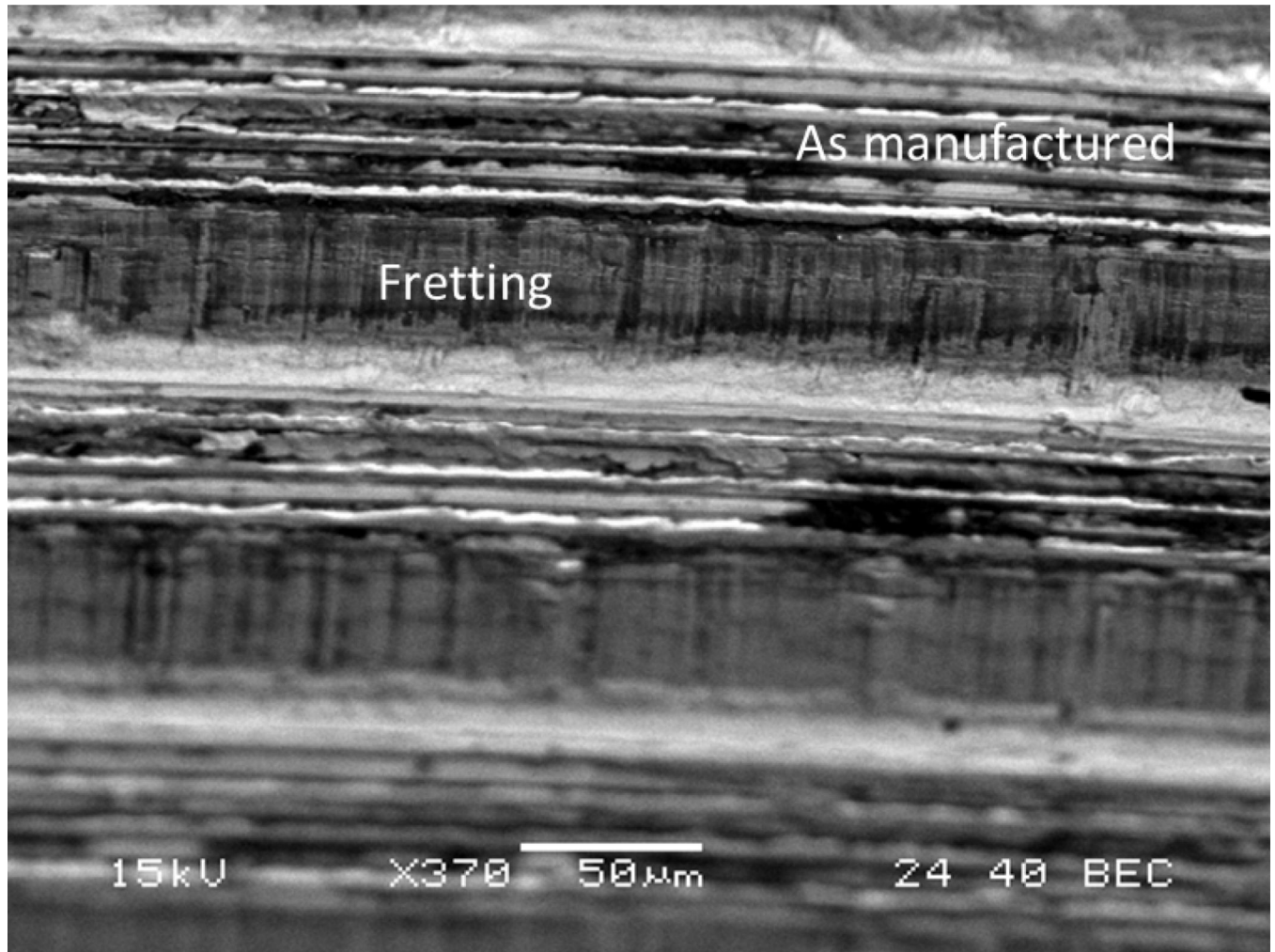
Figure 9.
SEM image taken in distal portion of metal head taper showing fretting in regions with
horizontal bands of material loss. Bands of material loss most likely corresponded to regions
in contact with trunnion as manufactured grooves (370×, BEC).
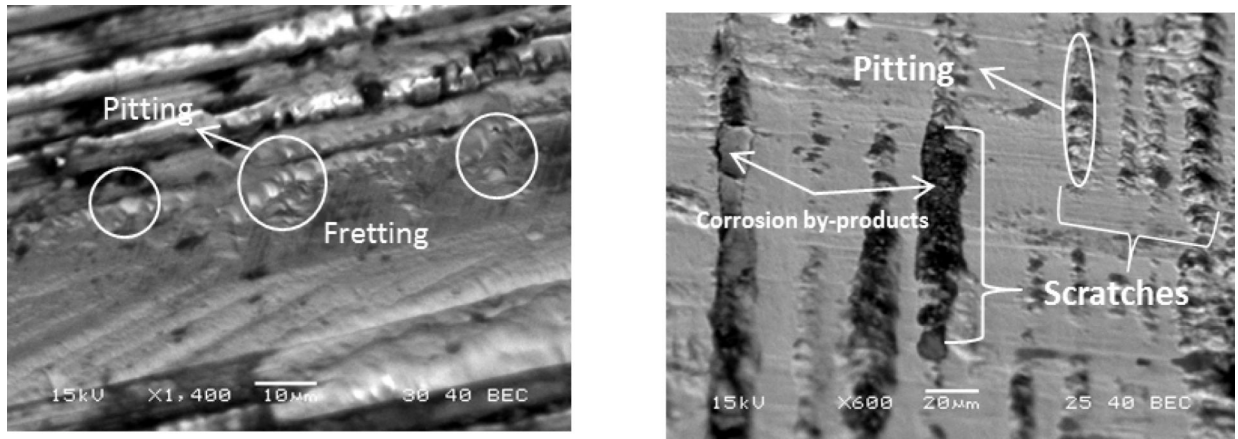
Figure 10.
A component showing pitting corrosion (marked in white circles) initiated preferentially in a crevice formed due to fretting abrasion (5–40μm scratches), imaged midway between proximal and distal ends on the taper (left, BEC, 1400×). A different component showing scratches (50–500μm) throughout head taper, with preferential pitting inside the scratches, imaged midway between proximal and distal ends on the taper (right, BEC, 600×). Corrosion by-products (biological and electrochemical deposits) have accumulated inside the scratches.
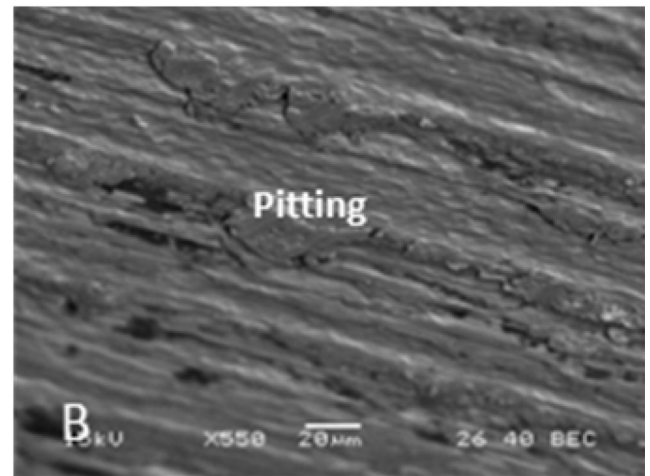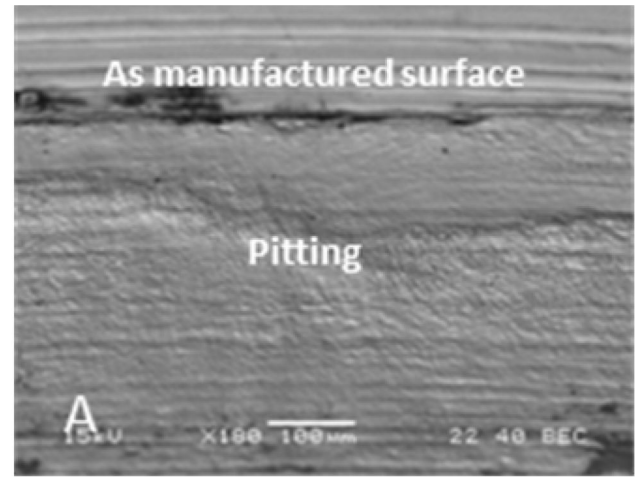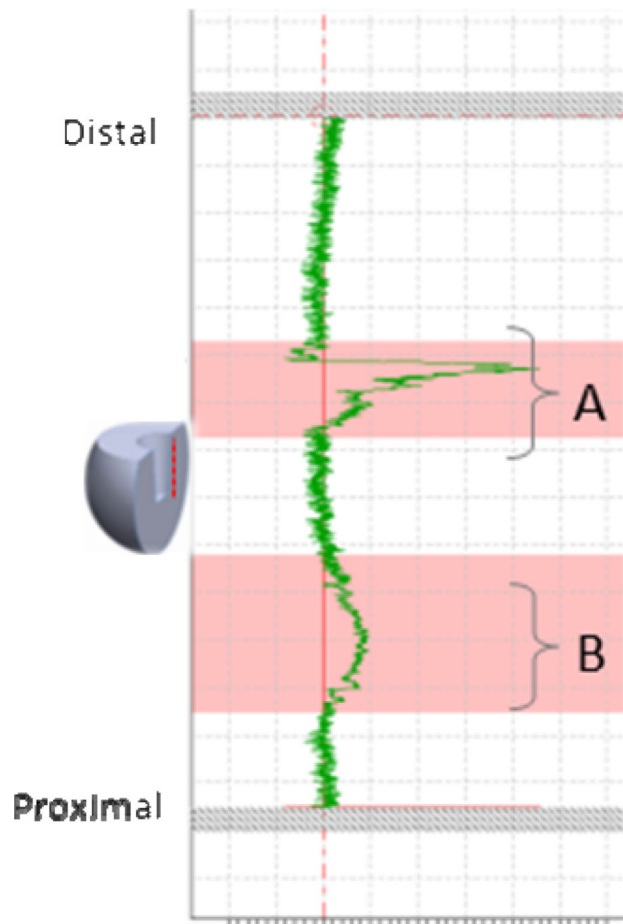
Figure 11.
Axial profile of a metal head implanted with a trunnion with a "smooth" finish (left).
Regions corresponding to the material loss, marked A and B were imaged using the SEM
(right). Both regions of material loss on the Talyrond profile showed evidence of change to
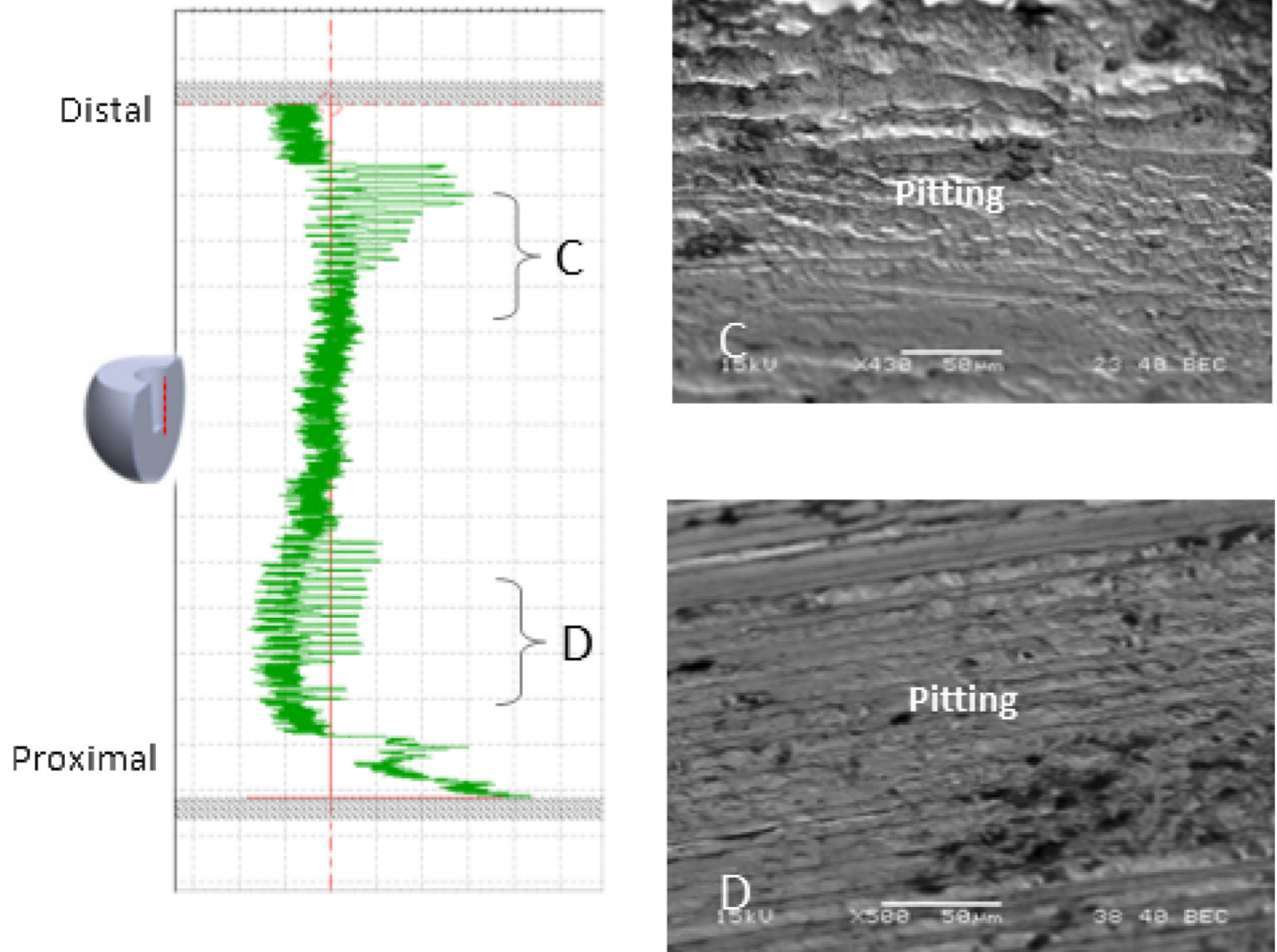the as manufactured surface.

Figure 12.
Axial profile of a metal head implanted with a "microgrooved" trunnion finish (left).
Regions corresponding to the material loss, marked C and D were imaged using the SEM
(right). Both regions of material loss on the Talyrond profile showed evidence of change to
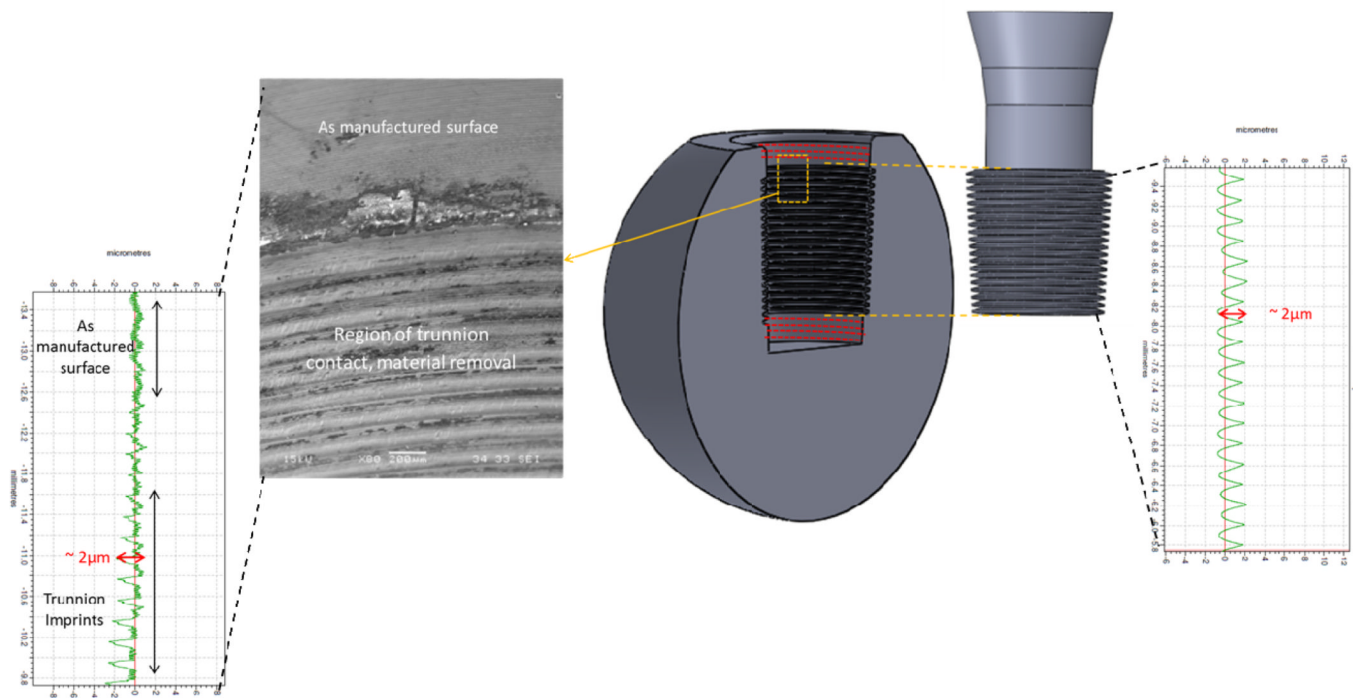the as manufactured surface.

Figure 13.
Schematic diagram showing the taper-trunnion interface and typical SEM image and measured profiles from head taper mated with microgrooved trunnion. The red dotted-lines represent locations used for roundness profile measurements.